RFC2-HA were treated with a more extensive panel of DNA-damaging agents for 8 h and proteins in resulting chromatin fractions were analyzed by immunoblotting with the anti-RFC2 antibody (Fig. 1E, upper panel). DNA damaging agents we tested included alkylating agents (EMS and MNNG), an oxidizing agent (H_2O_2), a DNA crosslinking agent (MMC), double strand break inducing agents (Bleomycin and IR) and the topoisomerase I inhibitor camptothecin (CPT). Of the genotoxic agents tested, only EMS, MNNG and H_2O_2 induced the shifted RFC2 band evident in MMS-treated cells (Fig. 1E, upper panel, lanes 7-10). Many of the agents failing to induce the RFC2 bandshift nevertheless induced very robust PCNA mono-ubiquitylation (Fig. 1E, lower panel). Therefore, we conclude that RFC2 modification is a specific response to a subset of genotoxins.

RAD18-dependent ubiquitylation of human RFC2. To test whether the shifted RFC2-specific band in MMS-treated cells was due to ubiquitylation, RFC2-HA was co-expressed with Flag-tagged ubiquitin in 293A cells. The transfected cells were treated with MMS. Endogenous and HA-tagged RFC2 proteins were immunoprecipitated with anti-RFC2 antibody from cell lysates, and the precipitated proteins were immunoblotted with either anti-RFC2 (Fig. 2A upper panel) or anti-Flag antibody to detect Flag-ubiquitin-modified proteins (lower panel). Anti-RFC2-reactive bands migrating at the sizes expected for mono-ubiquitylated RFC2 (48 kDa) were observed in our anti-RFC2 immunoprecipitates (Ub-RFC2 in lanes 3 and 4). In addition to the 48 kDa Ub-RFC2 band, extra two slowly migrating bands (51 and 62 kDa) were observed in the immunoprecipitates obtained from cells transfected with Flag-tagged ubiquitin (Flag-Ub-RFC2 in lane 4), which were also detectable by immunoblotting with anti-Flag antibody (lane 8). From these results we conclude that the slow migrating forms of RFC2 in MMS-treated cells are ubiquitylated species.

In *S. cerevisiae* and human cells, mono-ubiquitylation of PCNA is dependent on the Rad18 E3-ubiquitin ligase (22,24,25). To determine whether ubiquitylation of RFC2 was similarly dependent on RAD18, RFC2 modification was tested in RAD18-overexpressing 293A cells (Fig. 2B) and *RAD18*-deficient HCT116 cells (Fig. 2C). As shown in Fig. 2B, over-expression of RAD18 induced the ubiquitylation of RFC2-HA and PCNA even in the absence of MMS treatment. Conversely, MMS-induced ubiquitylated forms of RFC2 decreased considerably (by 50%) in HCT116 $RAD18^{-/-}$ cells compared to those in matched HCT116 $RAD18^{+/+}$ cells (Fig. 2C). These results suggest that RFC2 mono-ubiquitylation in MMS-treated cells is mediated, at least in large part by RAD18, most probably as a complex with RAD6. Interestingly, RAD18-overexpression

also induced chromatin accumulation of RFC2 (Fig. 2B). Ubiquitylation and chromatin accumulation of RFC2 (and also RFC4) was observed in response to MMS treatment and Rad18-overexpression. Because MMS treatment induced chromatin accumulation of each RFC subunit (Fig. 1A), it is most likely that increased chromatin loading of the entire RFC complex occurs in response to MMS.

A RFC2 mutant is ubiquitylated in the absence of DNA damage. It has been reported that the RFC2(p40) subunit of human RFC binds the large subunit of RPA (11). In *S. cerevisiae*, a mutation in *rfc4* (yeast homolog of human *RFC2(p40)*) was found to display synthetic lethality with mutation in the gene encoding Rpa1 (the large subunit of *S. cerevisiae* RPA) (40). Interestingly, this mutant Rfc4(p40) showed weaker physical interaction with RPA than the wild type Rfc4(p40). This mutation, resulting in an amino acid change of aspartate to asparagine at residue 201, maps to the RFC box VIII, which is one of the conserved motifs found in all RFC subunits (16,41). The D201 residue of *S. cerevisiae* Rfc4 is conserved and found at an identical position in RFC2 from higher eukaryotes, including humans (Fig. 3A). We replaced D228 of human RFC2 (which corresponds to *S. cerevisiae* Rfc4 D201) with an asparagine residue (D228N) or an alanine (D228A). HA-tagged forms of mutant or wild-type RFC2 were expressed in 293A cells by transfection (Fig. 3B). The wild-type and mutant forms of RFC2-HA were expressed at similar levels; however, while the wild-type and D228N mutant RFC2 proteins showed no ubiquitylation of RFC2, the D228A mutant RFC2 protein underwent extensive modification without any genotoxin treatment (Fig. 3B, lane 8). The multiple shifted bands of RFC2 D228A decreased by 55% in HCT116 *RAD18*$^{-/-}$ cells compared to those in matched HCT116 *RAD18*$^{+/+}$ cells (Fig. 3C). Therefore, we conclude that the multiple Rad18-dependent species we observed correspond to mono- and poly-ubiquitylated forms of RFC2. As described in the previous sections, we observed mono-ubiquitylated forms of the wild-type RFC2-HA in MMS-treated cells, but did not observe high levels of its poly-ubiquitylated forms. The results of Fig. 3B indicate that the RFC2 D228A mutant is extensively ubiquitylated and accumulates as multiple poly-ubiquitylated species (even in the absence of genotoxin treatments) when ectopically expressed. Although the difference in susceptibility to spontaneous ubiquitylation between D228A and D228N is unexpected, by analogy with the *S. cerevisiae* Rfc4 D201N mutant protein, it is most likely that D228 of human RFC2 is also involved in interaction with RPA. While we have not formally verified the reduced interaction of human RFC D228A with RPA, we infer that RAD6-RAD18-mediated RFC2 ubiquitylation is regulated by interaction with RPA (see below).

RFC2 is modified by the RAD6-RAD18 complex in vitro. We subsequently examined whether RFC2 could be modified by the RAD6-RAD18 complex *in vitro*. Recombinant RFC complex, (including RFC1-5 proteins of human origin), was expressed in *E. coli* and then purified. Mono-ubiquitylation of RFC2 *in vitro* was investigated by mixing the RFC1-5 complex with purified recombinant RAD6A (E2 ubiquitin-conjugating enzyme)-RAD18 (E3 ubiquitin ligase) complex. As shown in Fig. 4, RFC2 was monoubiquitylated *in vitro* when incubated in the presence of purified RAD6A and RAD18 plus ubiquitin and its activating enzyme (lane 2), although at a much lower efficiency when compared with PCNA. It should also be noted that the *in vitro* modification of RFC2 generated only a single mono-ubiquitylated species while at least two mono-ubiquitylated forms of RFC2 (corresponding to mono-ubiquitylation at different residues) resulted from MMS treatment of intact cells. The reason for the differential patterns of RAD18-mediated RFC2 mono-ubiquitylation observed *in vitro* and in intact cells is not yet clear, but could result from the existence of additional RFC2-directed E3 ligases *in vivo*. The difference also indicates that *in vitro* assay conditions do not fully recapitulate the complexity of events involved in RPA-sensitive RFC2 ubiquitylation at stalled replication forks *in vivo*. It should be noted that our *in vitro* assay uses primed M13 ssDNA, which mimics the leading strand synthesis rather than the lagging strand synthesis that requires the RFC complex more frequently. PCNA did not affect RFC2 mono-ubiquitylation (lane 4), although the modification was dependent on the presence of DNA (data not shown). Interestingly, however, the addition of RPA inhibited RAD6-RAD18-dependent mono-ubiquitylation completely (lanes 3 and 5). In parallel reactions, RPA did not affect the mono-ubiquitylation of PCNA (lanes 4 and 5). Therefore, RPA specifically inhibits RAD18-dependent mono-ubiquitylation of RFC2. The inhibition of RAD18-mediated RFC2 ubiquitylation by RPA *in vitro* is consistent with our finding that the RFC2 D228A mutant is more extensively modified than wild-type RFC2 in intact cells.

DISCUSSION

Protein ubiquitylation is critical for numerous cellular functions, including DNA damage response pathway. In this report we have demonstrated that RFC2 is ubiquitylated in human cells via DNA damage-independent and genotoxin-inducible mechanisms. RFC2 ubiquitylation is partially dependent on RAD18 as demonstrated by the decreased MMS-induced RFC2 ubiquitylation in *RAD18*$^{-/-}$ cells compared to matched *RAD18*$^{+/+}$ HCT116 cells (Fig. 2C). Conversely, RFC2 undergoes genotoxin-independent mono-ubiquitylation in cells over-expressing RAD18.

RAD18-dependent mono-ubiquitylation of RFC2 was also verified by *in vitro* reaction (Fig. 4). The RAD18-induced ubiquitylation of RFC2 *in vitro* and in RAD18-over-expressing cultured cells is similar to what we and others have observed for PCNA, a bona fide RAD18 substrate. These results are further indicative of a direct E3 ligase-substrate relationship between RAD18 and RFC2.

Our *in vitro* experiments clearly show an inhibitory effect of RPA on RFC2 mono-ubiquitylation (Fig. 4). The involvement of RPA in regulation of RFC2 ubiquitylation *in vivo* is also suggested by our experiments with the RFC2-D228A mutant (corresponding to a *S. cerevisiae* RPA interaction-deficient Rfc4 mutant). We have shown that RFC2-D228A undergoes DNA damage-independent ubiquitylation, which is reduced substantially in RAD18-deficient cells (Fig. 3C). Our *in vitro* assay for RAD6-RAD18-dependent RFC2 ubiquitylation does not completely recapitulate all aspects of RFC2 modification *in vivo*, and the role of RFC2 D228 in mediating RPA associations is not yet clear. However, our results strongly suggest a key regulatory role of RPA in RFC2 ubiquitylation. We propose that Rad18-dependent RFC2 ubiquitylation is repressed by RPA in undamaged cells, and that de-repression of RFC2 ubiquitylation occurs following MMS-induced DNA damage.

Our experiments also indicate that the RFC2-D228A mutant is subject to extensive poly-ubiquitylation. It is likely that poly-ubiquitylated RFC2 is generated by linkage of additional ubiquitin molecules to lysine residues that are first mono-ubiquitylated by RAD18. By analogy, following genotoxin treatments PCNA is mono-ubiquitylated by RAD6-RAD18 on lysine-164, and subsequently the mono-ubiquitylated PCNA is poly-ubiquitylated in a reaction mediated by MMS2-UBC13 and RAD5 (22,23,42,43). It will be interesting to determine whether RAD5 or alternative E3 ligases contribute to the RAD18-initiated poly-ubiquitylation of RFC2. Mono-ubiquitylated and poly-ubiquitylated species of PCNA promote different damage response pathways, error-prone and error-free post-replication repair (PRR), respectively. It will be interesting to determine whether the mono- and poly-ubiquitylated species of RFC2 similarly serve distinct effector functions. Several studies have demonstrated that a residual level of PCNA ubiquitylation is detectable in RAD18-deficient cells. Similarly, we have shown that RAD18-deficiency does not completely ablate RFC2 ubiquitylation. Clearly, further work is necessary to identify the E3 ligases involved in RAD18-independent ubiquitylation of PCNA and RFC2.

In order to obtain insight into the question of why the RFC2 D228A mutant is susceptible to ubiquitylation without DNA damage, we constructed tertiary structure models of human RFC2 (Fig. 3A) and RFC complex bound to

PCNA (Fig. 5) by homology modeling using the reported yeast structure (41) as the template. Each RFC subunit contains three structurally conserved domains (Domain I, II and III). Domains I and II comprise an ATPase module of the AAA+ family, which is connected by a flexible linker to another helical domain (Domain III). Our structural model revealed that D228 resides in the turn between helix14 and helix15 (Sensor 2 helix), which is located near the hinge region between Domain II and III (Fig. 5C). This implies that RFC2-D228 is not exposed to the outer surface, but instead is buried in the spiral structure. It is unlikely, therefore, that the D228 residue directly associates with RPA, as long as such a tight RFC-PCNA complex is maintained.

Whether the RFC complex remains around primed end following PCNA loading is controversial (11,30,44-46). However, the RFC complex may stay associated with PCNA in a structure different from the tight complex as shown in Fig. 5A, which allows RPA to associate with RFC2 around the D228 residue. Another possibility is that the D228A mutation causes a conformational change in the RFC complex structure, possibly altering interactions with RPA and affecting susceptibility to ubiquitylation.

It is notable that RFC2 is ubiquitylated in human cells following treatment with alkylating agents, but not in response to genotoxins that induce DSB, bulky adducts, ICL, or nucleotide depletion. Therefore, it appears that RFC2 mono-ubiquitylation is due to a specific alteration in DNA structure induced by alkylating agents or to a specific DNA repair intermediate. Identification of DNA structure(s) responsible for RFC2 ubiquitylation may provide insight into consequences of DNA damage due to particular genotoxins. Alkylating agents modify DNA by adding methyl or ethyl groups to a number of nucleophilic sites on the DNA bases (47). The predominant adduct in double strand DNA resulting from MMS or MNNG exposure is 7-methylguanine (*N*7-MeG) and 3-methyl adenine (*N*3-MeA). *N*3-MeA blocks replication, whereas *N*7-MeG does not block replication or miscode. Another deleterious adduct is ^{6}O-methyl guanine (^{6}O-MeG). ^{6}O-MeG is produced relatively lower level compared to *N*7-MeG and *N*3-MeA, but highly mutagenic and toxic, since ^{6}O-MeG-T mispairing not only results in G/C to A/T transition but also is recognized by mismatch repair (MMR) in process that is a potent signal of apoptosis (48). However, the human kidney cell line 293A cells, used in this study, are MMR-deficient, due to epigenetic silencing of the *hMLH1* gene by promoter hypermethylation (49). Therefore. ^{6}O-MeG is not the lesion responsible for RFC2 monoubiquitylation and instead *N*7-MeG and/or *N*3-MeA are the likely candidates. Treatment of 293A cells with an oxidative agent (H_2O_2) also induced RFC2 monoubiquitylation (Fig. 1E).

Base excision repair (BER) is the common pathway for repairing *N*7-MeG, *N*3-MeA and oxidative damage (47,50,51). BER is initiated with removal of altered bases by DNA-glycosylase. The resulting apurinic/apyrimidinic (AP) sites are nicked and repair is completed by re-synthesis and ligation. Therefore, for proficient BER, a proper balance of the individual steps involved in DNA repair is important. Imbalanced BER may result in deleterious intermediates, such as AP sites. Furthermore, methylation or oxidation of purines destabilizes the *N*-glycosyl bond, thus rendering the base more susceptible to hydrolysis to form an AP site. Therefore, AP sites are the lesions most likely to cause RFC2 monoubiquitylation, although precisely how RPA-RFC2 interaction is affected at AP sites is unclear.

Another possible role of RFC2 ubiquitylation is as the sensing signal for damage recognition. The RFC1-5 complex (containing RFC2) has several functions. During normal DNA replication RFC1-5 acts as clamp loader for PCNA, whereas in the DNA damage response RAD17-RFC2-5 loads the 9-1-1 complex. At present we do not know whether loading of PCNA, the 9-1-1 complex, or both is affected by RAD18-dependent RFC2 modification. Experiments to further address the significance of RFC2 modification and to identify relevant effectors of modified RFC are underway.

REFERENCES

1. Hartwell, L. H., and Weinert, T. A. (1989) *Science* **246**(4930), 629-634
2. Carr, A. M. (2002) *DNA Repair (Amst)* **1**(12), 983-994
3. Kastan, M. B., and Bartek, J. (2004) *Nature* **432**(7015), 316-323
4. Sancar, A., Lindsey-Boltz, L. A., Unsal-Kacmaz, K., and Linn, S. (2004) *Annu. Rev. Biochem.* **73**, 39-85
5. Bochkareva, E., Korolev, S., Lees-Miller, S. P., and Bochkarev, A. (2002) *EMBO J.* **21**(7), 1855-1863
6. Binz, S. K., Sheehan, A. M., and Wold, M. S. (2004) *DNA Repair (Amst)* **3**(8-9), 1015-1024
7. Kelman, Z., and O'Donnell, M. (1995) *Nucleic Acids Res.* **23**(18), 3613-3620
8. Wyman, C., and Botchan, M. (1995) *Curr. Biol.* **5**(4), 334-337
9. Fien, K., and Stillman, B. (1992) *Mol. Cell. Biol.* **12**(1), 155-163
10. Krishna, T. S., Kong, X. P., Gary, S., Burgers, P. M., and Kuriyan, J. (1994) *Cell*

79(7), 1233-1243

11. Yuzhakov, A., Kelman, Z., Hurwitz, J., and O'Donnell, M. (1999) *EMBO J.* **18**(21), 6189-6199
12. Tsurimoto, T., and Stillman, B. (1991) *J. Biol. Chem.* **266**(3), 1961-1968
13. Maga, G., and Hubscher, U. (2003) *J. Cell. Sci.* **116**(Pt 15), 3051-3060
14. Warbrick, E. (2000) *Bioessays* **22**(11), 997-1006
15. Zou, Y., Liu, Y., Wu, X., and Shell, S. M. (2006) *J. Cell. Physiol.* **208**(2), 267-273
16. Cullmann, G., Fien, K., Kobayashi, R., and Stillman, B. (1995) *Mol. Cell. Biol.* **15**(9), 4661-4671
17. Neuwald, A. F., Aravind, L., Spouge, J. L., and Koonin, E. V. (1999) *Genome Res.* **9**(1), 27-43
18. Kim, J., and MacNeill, S. A. (2003) *Curr. Biol.* **13**(22), R873-875
19. Majka, J., and Burgers, P. M. (2004) *Prog. Nucleic Acid Res. Mol. Biol.* **78**, 227-260
20. Zernik-Kobak, M., Vasunia, K., Connelly, M., Anderson, C. W., and Dixon, K. (1997) *J. Biol. Chem.* **272**(38), 23896-23904
21. Wu, X., Shell, S. M., and Zou, Y. (2005) *Oncogene* **24**(29), 4728-4735
22. Hoege, C., Pfander, B., Moldovan, G. L., Pyrowolakis, G., and Jentsch, S. (2002) *Nature* **419**(6903), 135-141
23. Stelter, P., and Ulrich, H. D. (2003) *Nature* **425**(6954), 188-191
24. Kannouche, P. L., Wing, J., and Lehmann, A. R. (2004) *Mol. Cell* **14**(4), 491-500
25. Watanabe, K., Tateishi, S., Kawasuji, M., Tsurimoto, T., Inoue, H., and Yamaizumi, M. (2004) *EMBO J.* **23**(19), 3886-3896
26. Friedberg, E. C., Lehmann, A. R., and Fuchs, R. P. (2005) *Mol. Cell* **18**(5), 499-505
27. Bienko, M., Green, C. M., Crosetto, N., Rudolf, F., Zapart, G., Coull, B., Kannouche, P., Wider, G., Peter, M., Lehmann, A. R., Hofmann, K., and Dikic, I. (2005) *Science* **310**(5755), 1821-1824
28. Shiomi, Y., Shinozaki, A., Nakada, D., Sugimoto, K., Usukura, J., Obuse, C., and Tsurimoto, T. (2002) *Genes Cells* **7**(8), 861-868
29. Fukuda, K., Morioka, H., Imajou, S., Ikeda, S., Ohtsuka, E., and Tsurimoto, T. (1995) *J. Biol. Chem.* **270**(38), 22527-22534
30. Masuda, Y., Suzuki, M., Piao, J., Gu, Y., Tsurimoto, T., and Kamiya, K. (2007) *Nucleic Acids Res.* **35**(20), 6904-6916
31. Henricksen, L. A., Umbricht, C. B., and Wold, M. S. (1994) *J. Biol. Chem.* **269**(15),

11121-11132

32. Honda, R., Tanaka, H., and Yasuda, H. (1997) *FEBS Lett.* **420**(1), 25-27
33. Imai, N., Kaneda, S., Nagai, Y., Seno, T., Ayusawa, D., Hanaoka, F., and Yamao, F. (1992) *Gene* **118**(2), 279-282
34. Harrison, S. D., Solomon, N., and Rubin, G. M. (1995) *Genetics* **139**(4), 1701-1709
35. Haas, A. L., and Bright, P. M. (1988) *J. Biol. Chem.* **263**(26), 13258-13267
36. Fiser, A., and Sali, A. (2003) *Methods Enzymol.* **374**, 461-491
37. Tomii, K., and Akiyama, Y. (2004) *Bioinformatics* **20**(4), 594-595
38. Koradi, R., Billeter, M., and Wuthrich, K. (1996) *J. Mol. Graph.* **14**(1), 51-55, 29-32
39. Bowman, G. D., Goedken, E. R., Kazmirski, S. L., O'Donnell, M., and Kuriyan, J. (2005) *FEBS Lett.* **579**(4), 863-867
40. Kim, H. S., and Brill, S. J. (2001) *Mol. Cell. Biol.* **21**(11), 3725-3737
41. Bowman, G. D., O'Donnell, M., and Kuriyan, J. (2004) *Nature* **429**(6993), 724-730
42. Motegi, A., Sood, R., Moinova, H., Markowitz, S. D., Liu, P. P., and Myung, K. (2006) *J. Cell Biol.* **175**(5), 703-708
43. Unk, I., Hajdu, I., Fatyol, K., Szakal, B., Blastyak, A., Bermudez, V., Hurwitz, J., Prakash, L., Prakash, S., and Haracska, L. (2006) *Proc. Natl. Acad. Sci. U. S. A.* **103**(48), 18107-18112
44. Gomes, X. V., and Burgers, P. M. (2001) *J. Biol. Chem.* **276**(37), 34768-34775
45. Podust, V. N., Tiwari, N., Stephan, S., and Fanning, E. (1998) *J. Biol. Chem.* **273**(48), 31992-31999
46. Moldovan, G. L., Pfander, B., and Jentsch, S. (2007) *Cell* **129**(4), 665-679
47. Wyatt, M. D., and Pittman, D. L. (2006) *Chem. Res. Toxicol.* **19**(12), 1580-1594
48. Stojic, L., Brun, R., and Jiricny, J. (2004) *DNA Repair (Amst)* **3**(8-9), 1091-1101
49. Trojan, J., Zeuzem, S., Randolph, A., Hemmerle, C., Brieger, A., Raedle, J., Plotz, G., Jiricny, J., and Marra, G. (2002) *Gastroenterology* **122**(1), 211-219
50. Hoeijmakers, J. H. (2001) *Nature* **411**(6835), 366-374
51. Krokan, H. E., Nilsen, H., Skorpen, F., Otterlei, M., and Slupphaug, G. (2000) *FEBS Lett.* **476**(1-2), 73-77

FOOTNOTES

We greatly appreciate the gift of the expression plasmids for human RPA, p11d-tRPA, from Dr. Marc

S. Wold (University of Iowa College of Medicine, Iowa City, Iowa) and mouse E1 expression vector RLC from Dr. Hideyo Yasuda (School of Life Science, Tokyo University of Pharmacy, and Life Science, Tokyo, Japan). The work was supported by grants-in aid for Scientific Research (A) and (B) from the Ministry of Education, Culture, Sports, Science and Technology, Japan.

The abbreviations used are: PCNA, proliferating cell nuclear antigen; RFC, replication factor C; pol, polymerase; RPA, replication protein A; EDTA, ethylenediaminetetraacetic acid; NP-40, Nonidet P-40; SDS-PAGE, sodium dodecyl sulfate poly-acrylamide gel electrophoresis; IR, ionizing radiation.

FIGURE LEGENDS

Figure 1. Accumulation of RFC-complex in chromatin fraction and modification of RFC2 following treatment of 293A cells with DNA damaging agents.

A. 293A cells transfected with a Flag epitope-tagged form of each subunit of RFC and RLCs were irradiated with UV (lane 3 and 9) or -ray (lane 6 and 12), or treated with DMSO (lane 1, 4, 7 and 10), MMS (lane 2 and 8) or HU (lane 5 and 11) for 8 h. Cell extracts recovered from transfected cells were then separated into chromatin (Chromatin; lanes 7-12) and soluble (Sup; lanes 1-6) fractions and analyzed by Western blotting with anti-Flag. Cell extracts recovered from RFC4-transfected cells were also analyzed by Western blotting with anti-tubulin or anti-histone H3 (lowest two blots).

B. 293A cells were irradiated with UV (lane 3) or -ray (lane 5), or treated with DMSO (lane 1), MMS (lane 2) or HU (lane 4) for 8 hr. Cell extracts recovered from transfected cells were then separated into chromatin (Chromatin) and soluble (Sup) fractions and analyzed by Western blotting either with anti-RFC1, anti-RAD17 or anti-RFC2. The arrowheads indicate the position of molecular weight marker (kDa).

C. 293A cells transfected with pCDNA3.RFC2-HA were treated with the indicated dose of MMS for 8 h. Chromatin fractions from the resulting cells were analyzed by immunoblotting with anti-RFC2 or anti-PCNA. The arrowheads indicate the position of molecular weight marker (kDa).

D. 293A cells transfected with pCDNA3.RFC2-HA were treated with 0.85 mM MMS for 1 hr (lanes 2-5) or UV-irradiated at 254 nm with 30 Jm^{-2} (lanes 6-9), and then incubated for the indicated times. Chromatin fractions were prepared and analyzed by Western blotting with anti-RFC2, anti-PCNA. Cells treated with DMSO (lane 1) are shown as control. The arrowheads indicate the position of molecular weight marker (kDa).

E. 293A cells transfected with pCDNA3.RFC2-HA were treated with various genotoxic agents.

Chromatin fractions were prepared and analyzed by Western blotting with anti-RFC2 or anti-PCNA. The arrowheads indicate the position of molecular weight marker (kDa).

Figure 2. RFC2 monoubiquitylation in response to DNA damaging agents is RAD18-dependent.

A. Lysates from RFC2-HA and Flag-Ubiquitin co-transfected 293A cells were analyzed by immunoprecipitation and Western blotting. pCDNA3.RFC2-HA was co-transfected either with pCDNA.Flag-Ubiquitin (lanes 4 and 8) or empty vector (lanes 3 and 7) in 293A cells. The following day, cells were treated with MMS for 8 h and then cell extracts were recovered. Cell extracts were immunoprecipitated with anti-RFC2 antibody. The resulting immune complexes were recovered using protein-A/G agarose and detected by immunoblotting with anti-RFC2 antibody (lanes 1-4) or anti-Flag antibody (lanes 5-8). Asterisks show nonspecific bands.

B. Western blot of lysates from 293A cells over-expressing hRAD18. pCDNA3. RFC2-HA was co-transfected either with pCAGGSh.RAD18 (lane 3) or empty vector (lane 2) in 293A cells. Chromatin fractions were prepared and analyzed by Western blotting with anti-RFC2 (lower panel) or anti-PCNA (upper panel). The arrowheads indicate the position of molecular weight marker (kDa).

C. Western blot of lysates from HCT116 cells (WILD) or *RAD18*-deficient HCT116 cells (*RAD18*$^{-/-}$). HCT116 cells transfected either with empty vector or pCAGGS.hRFC2 were treated with 0.85 mM MMS for 8 h. Chromatin fractions from the resulting cells were analyzed by immunoblotting with anti-RFC2 antibody. The arrowheads indicate the position of molecular weight marker (kDa).

Figure 3. DNA damage independent monoubiquitylation of hRFC2-D228A.

A. Schematic diagram and tertiary model of human RFC2 showing the location of D228 and the sequences of the surrounding regions. Corresponding sequences for *S. cerevisiae* RFC2(p40) and mouse RFC2 homologues are also shown. The conserved Sensor 2 helix is represented by box and the location of the conserved SRC motif is indicated as arrow. D228 of hRFC2, shown in red, corresponds to *S. cerevisiae* D201, which shows synthetic-lethality with mutation in Rpa-1(*rfa1*-Y29H). There are seven conserved RFC boxed numbered consecutively from N-terminus to C-terminus.

B. 293A cells were transfected with expression vectors encoding wild-type (lanes 2 and 6), D228N (lanes 3 and 7) or D228A (lanes 4 and 8) forms of hRFC2-HA. 24 hr after transfection cells were harvested and separated into chromatin (lanes 5-8) and soluble fractions (lanes 1-4) then immunoblotted with anti-RFC2 or anti-PCNA antibody. The arrowheads indicate the position of molecular weight marker (kDa).

C. Western blot of lysates from HCT116 cells (WILD) or *RAD18*-deficient HCT116 cells (*RAD18*$^{-/-}$). HCT116 cells transfected with pCAGGS.hRFC2(D228) were treated with 0.85 mM MMS for 8 h. Chromatin fractions from the resulting cells were analyzed by Western blotting with anti-RFC2 antibody. The arrowheads indicate the position of molecular weight marker (kDa).

Figure 4. *In vitro* mono-ubiquitylation of RFC2. *In vitro* ubiquitylation was carried out by mixing RFC with mouse E1, RAD18-RAD6A complex, ubiquitin and singly primed single stranded M13 mp18 DNA in the presence or absence of RPA or PCNA as indicated. The reaction products were analyzed by Western blotting with anti-RFC2 or anti-PCNA antibody.

Figure 5. A model for human clamp-loader/clamp complex. Ribbon (RFC2) and wire (Ca-trace, RFC1, RFC3-5 and PCNA) representations of the homology model for human RFC1-5 / PCNA complex. The five subunits of each clamp loader complex are denoted. The colors for each subunits are as follows with the helical collar domains (gray) at the top of the figure; RFC1, pink; RFC2, navy; RFC3, red; RFC4, green; RFC5, orange; PCNA, gold. The side-chain atoms of Asp228 of RFC2 are indicated as balls in cyan. A. A side view of the clamp-loader/clamp complex in which RFC2 is in the front. B. Views from the DNA-interacting pore of the clamp loader subunits. Domain I and II of AAA+-domain and 14 and 15 of RFC2 are indicated.

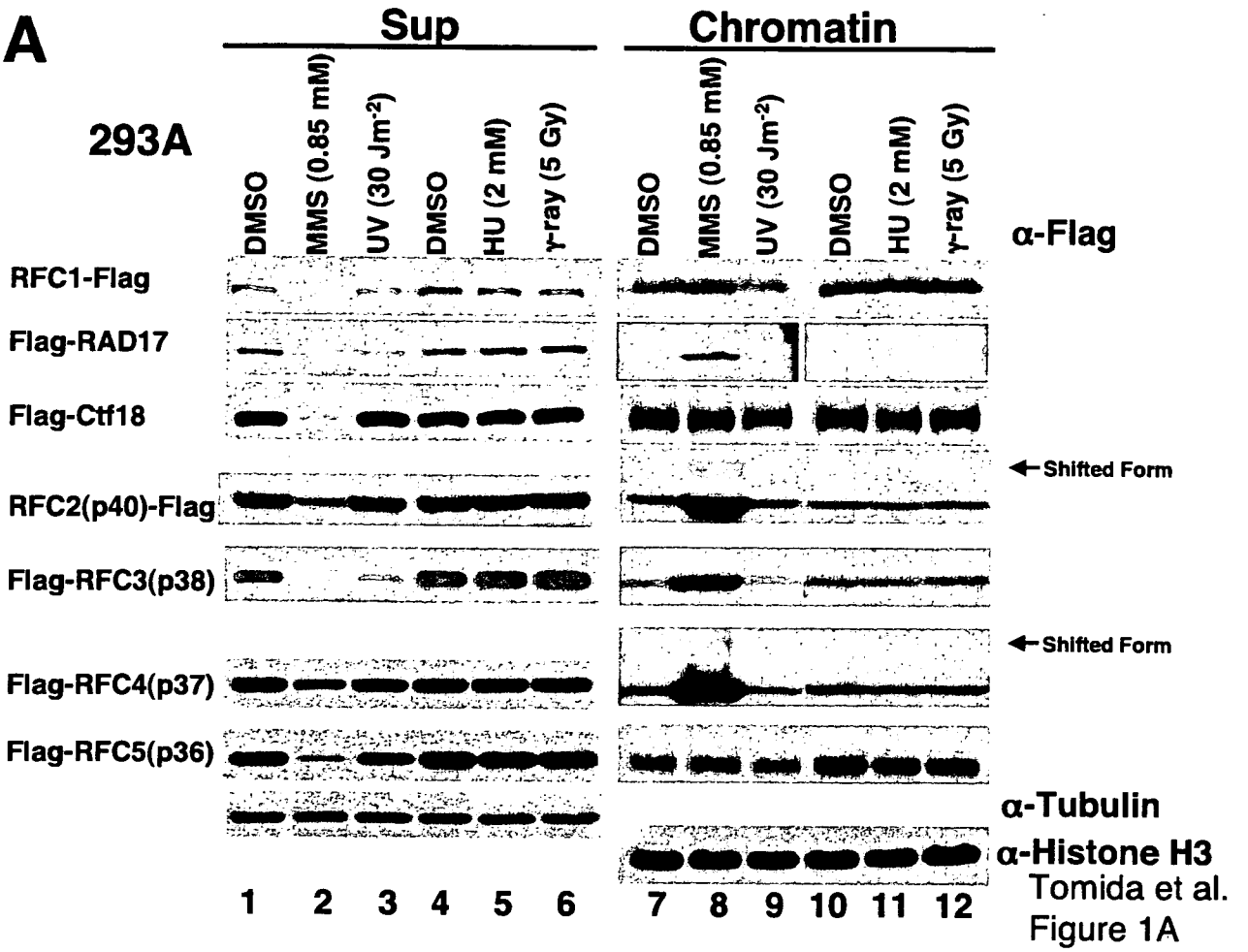

Tomida et al.
Figure 1A

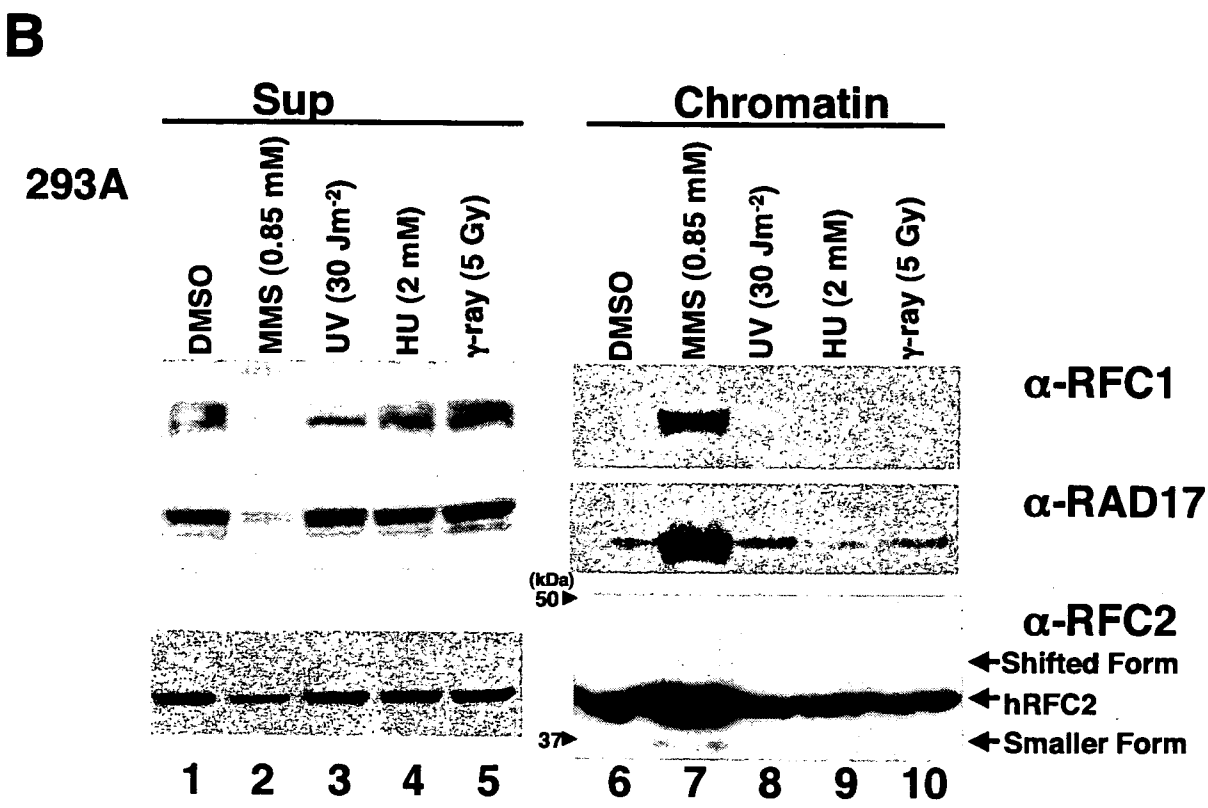

Tomida et al. Figure1B

C

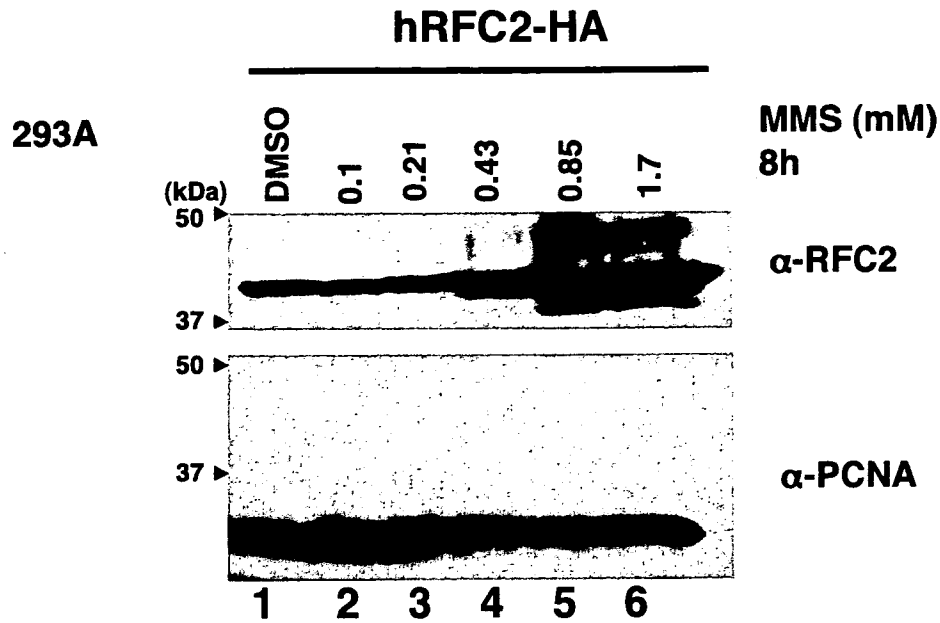

Tomida et al. Figure 1 C

D

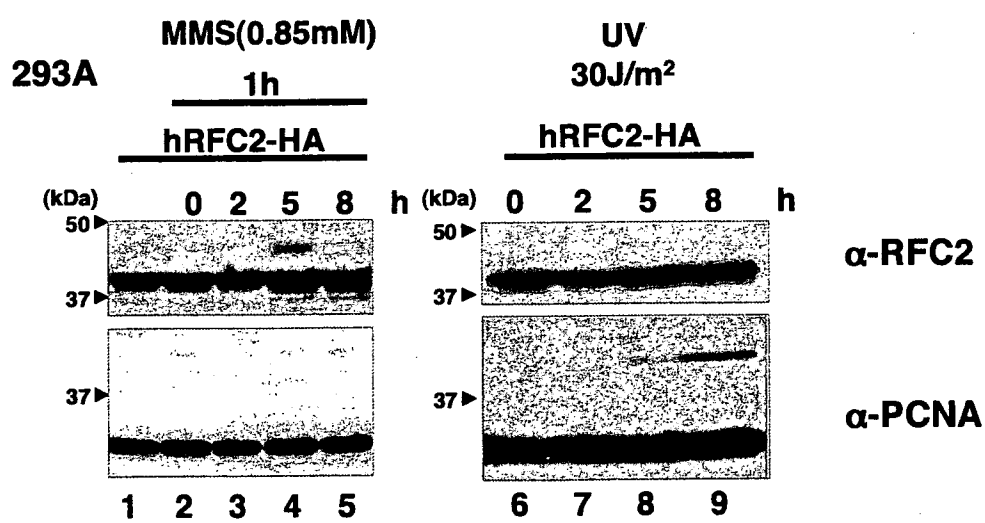

Tomida et al. Figure 1 D

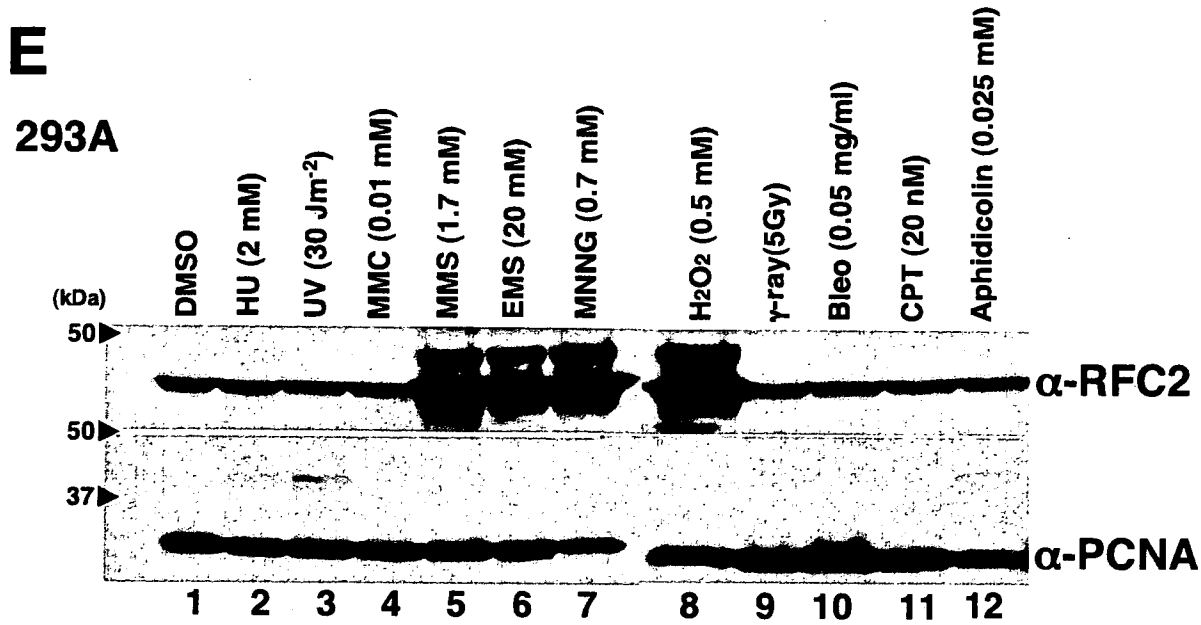

Tomida et al. Figure 1E

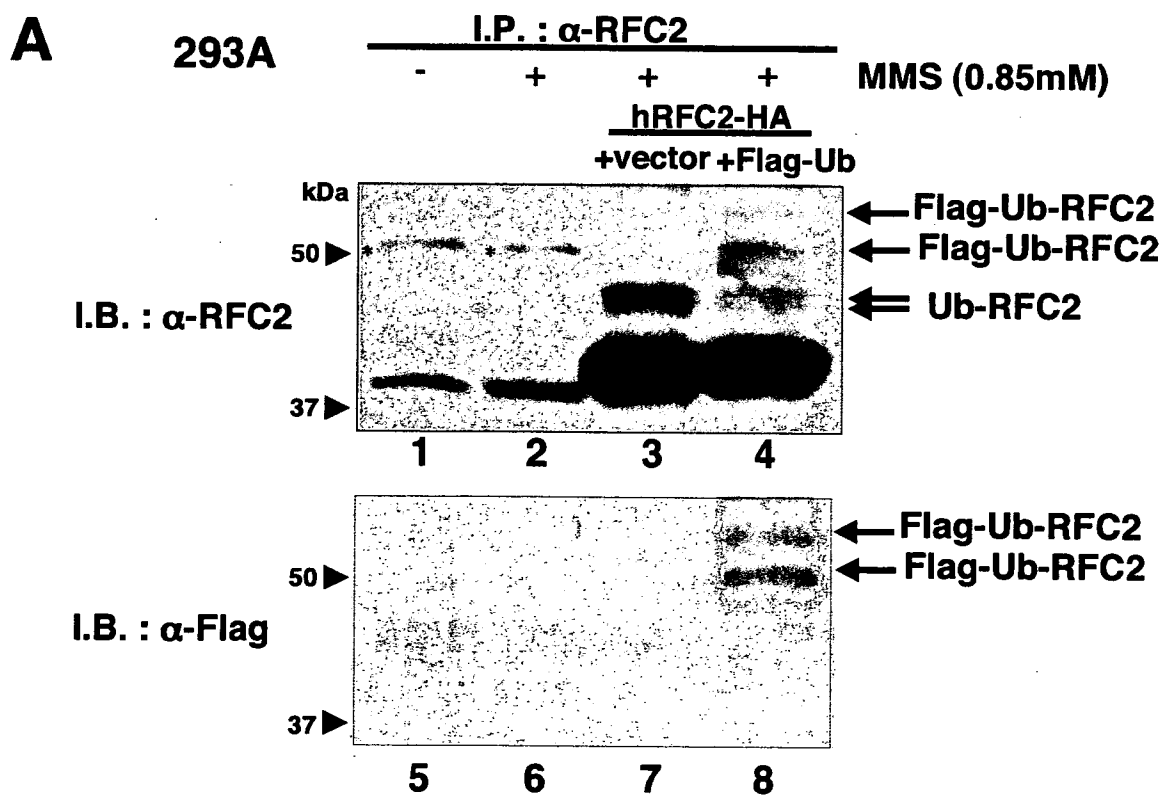

Tomida et al. Figure 2A

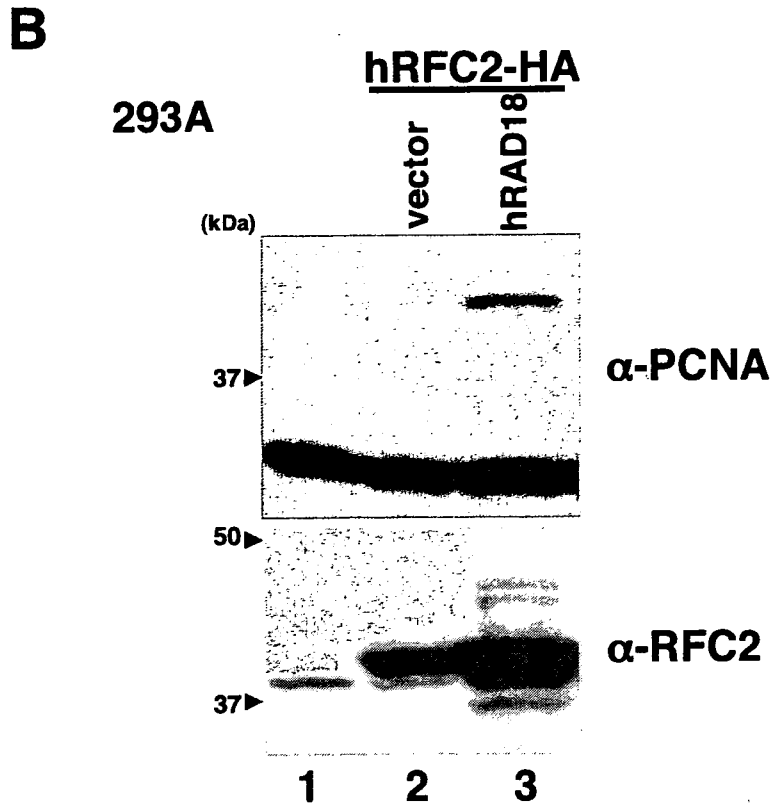

Tomida et al. Figure 2B

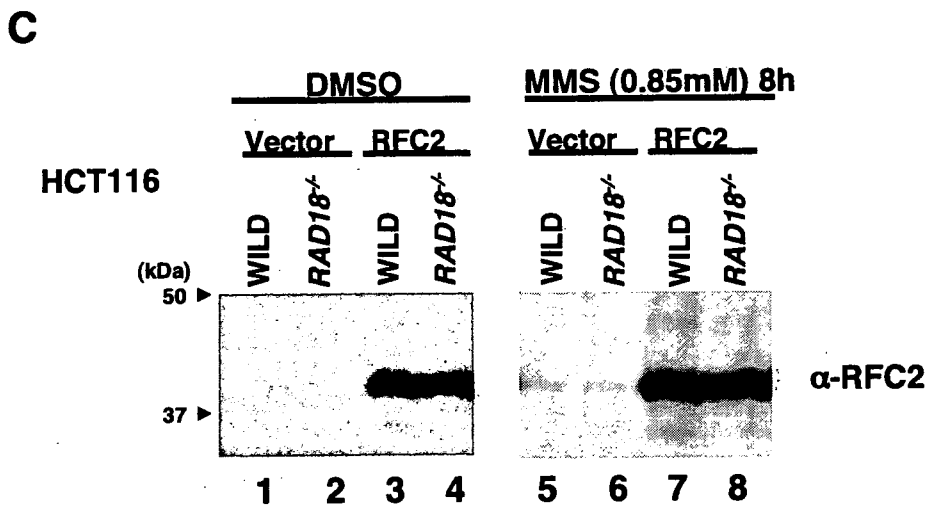

Tomida et al. Figure 2C

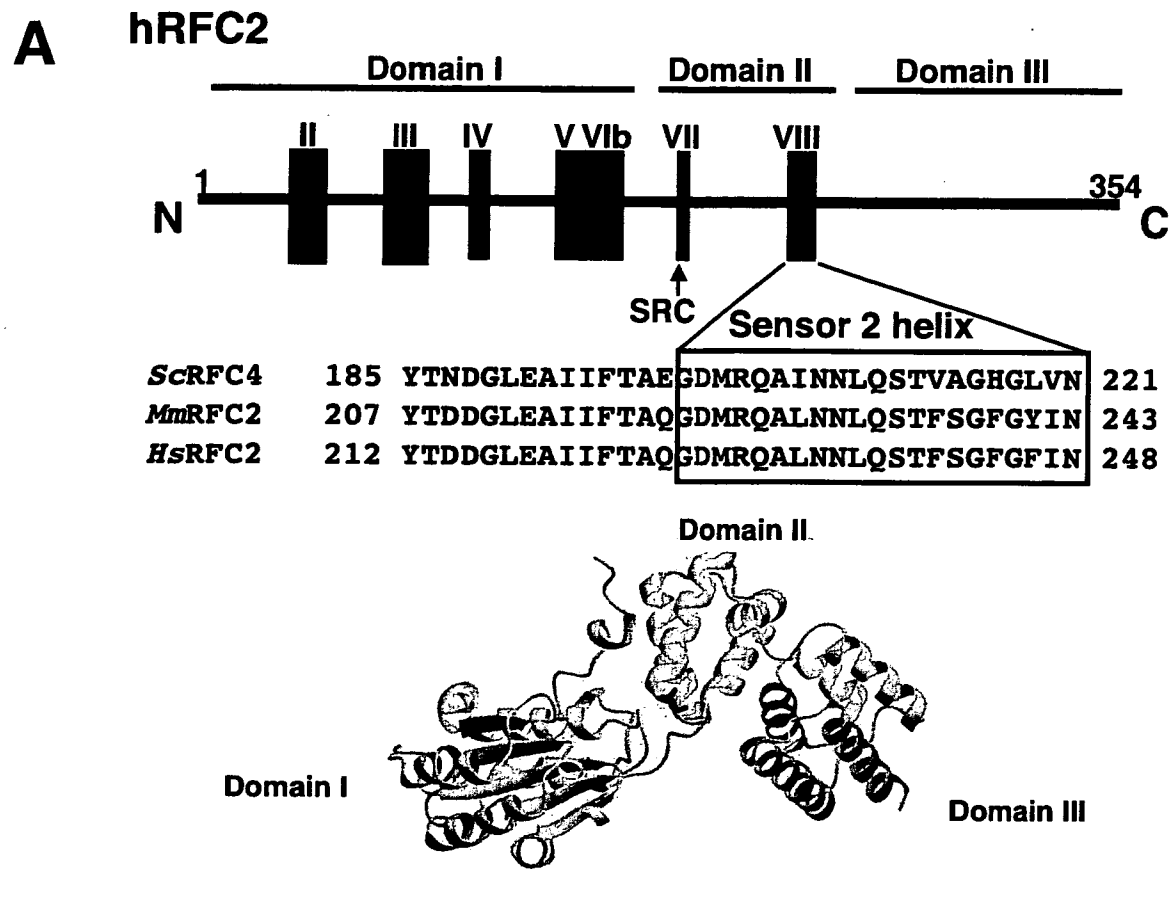

Tomida et al. Figure 3A

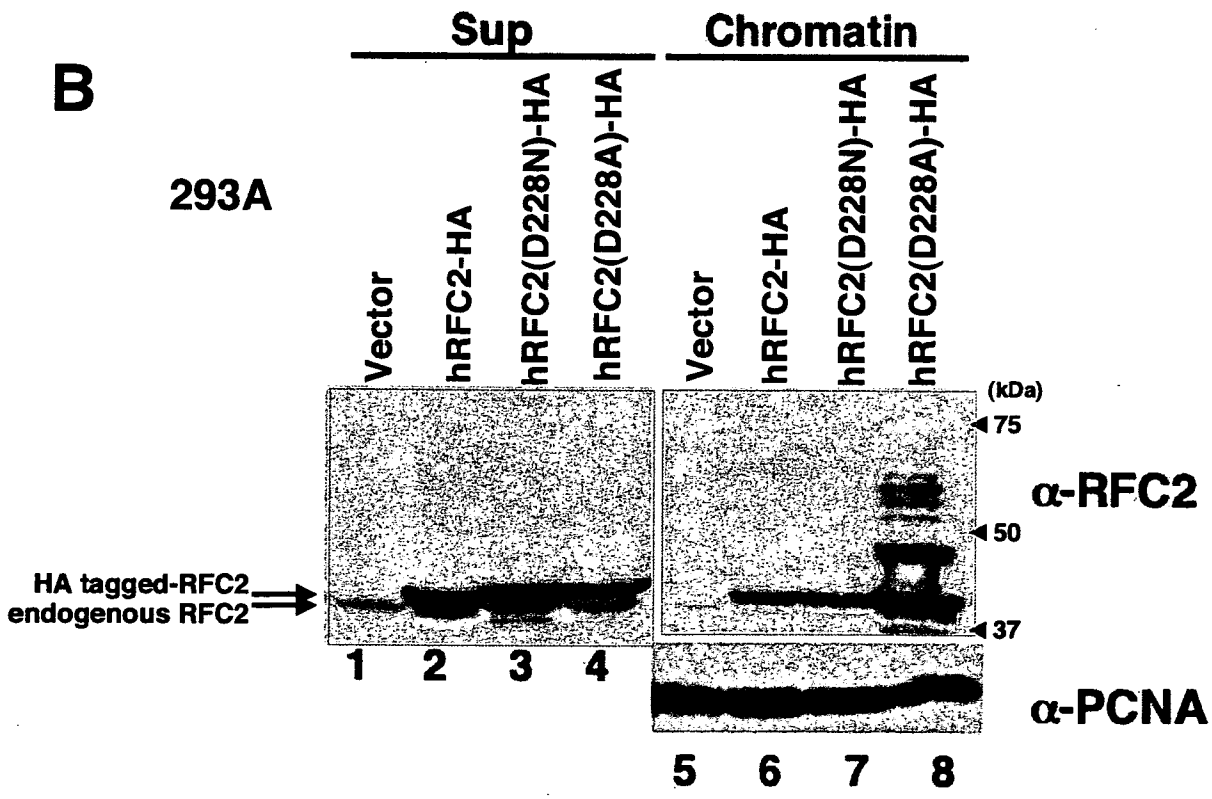

Tomida et al. Figure 3B

C

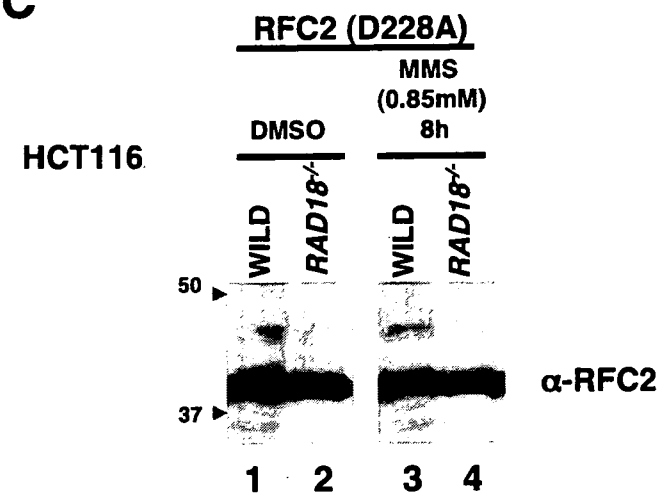

Tomida et al. Figure 3C

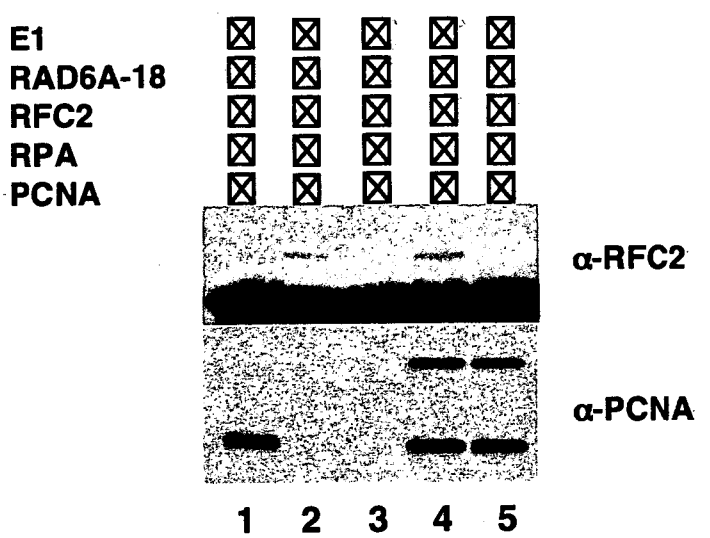

Tomida et al. Figure 4

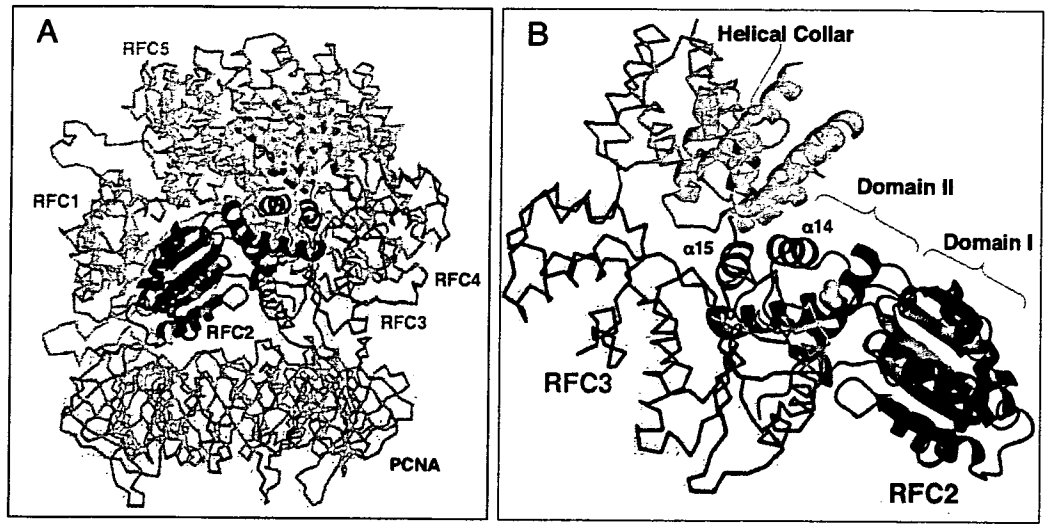

Tomida et al. Figure 5

J. Radiat. Res., 48, 205–210 (2007)

Regular Paper

Tumor Induction by Monoenergetic Neutrons in B6C3F1 mice

Hiromitsu WATANABE[1]*, Naoki KASHIMOTO[1], Junko KAJIMURA[1], Masayori ISHIKAWA[2] and Kenji KAMIYA[1]

Monoenergetic neutrons/Tumor induction/Mouse.

This study was undertaken to investigate induction of tumors by monoenergetic neutrons in B6C3F1 mice. Individual groups of 6 week-old animals of both sexes (about 30 mice/group) were exposed to 0.5 Gy of various monoenergetic neutrons (dose rate 0.5 cGy/min) and then observed for 13 months. The incidences of tumors (mainly liver neoplasms) in non-irradiated male and female controls were 11% and 0%, respectively. In the irradiated animals, the incidences were 53%, 50%, 60% and 43% in males, and 75%, 81%, 71%, and 85% in females, after 0.18, 0.32, 0.6 and 1.0 MeV neutron exposure, respectively. There were no significant differences in the tumor induction rate among the different energy groups.

INTRODUCTION

The biological effects of monoenergetic neutrons are of clear interest to basic science and radiation protection, as evidenced by a number of reports of *in vitro* studies.[1–11] To our knowledge, however, there has been relatively little work on the genetic effects of monoenergetic neutrons at various energy levels *in vivo*. In order to study the radiobiological effects of neutrons, the Hiroshima University Radiobiological Research Accelerator (HIRRAC) can be operated under conditions of high proton beam currents of 1mA and acceleration voltages up to 3 MeV. Neutron irradiation is possible in the energy range from 0.07 to 1.13 MeV using a lithium target.[12,13]

Specifications for biological irradiation cover monoenergetic beam conditions, dose rates and deposited energy spectra. High dose rates of monoenergetic neutron fields are useful for studying the neutron energy dependence of biological effects, and also the basic mechanisms of action of neutrons. Monoenergetic neutrons which have a narrow neutron spectrum are particularly useful in this regard. Therefore the present study was undertaken to investigate their long-term biological effects in mice, with the focus on tumor development.

*Corresponding author: Phone: +082-257-5893,
Fax: +082-257-5843,
E-mail: tonko@hiroshima-u.ac.jp

[1]Department of Experimental Oncology, Research Institute for Radiation Biology and Medicine, Hiroshima University 1-2-3 Kasumi, Minami-ku, Hiroshima, 734-8553, Japan. [2]Department of Medical Physics, Hokkaido University Hospital North 15 West 7, Kita-ku, Sapporo,060-8648, Japan

doi:10.1269/jrr.0614

MATERIALS AND METHODS

Animals

Crj:B6C3F1 mice of both sexes were purchased from Charles River Japan Inc. (Hino, Japan) and housed about five per autoclaved cage on sterilized wood chips, in a room with controlled temperature (24 ± 2°C) and humidity (55 ± 10%) under a regular 12-h light, 12-h dark cycle. The animals were maintained according to the 'Guide for Care and Use of Laboratory Animals' established by Hiroshima University. All mice received a normal diet MF (Oriental Yeast Co. Ltd., Tokyo) and tap water *ad libitum*. The experimental protocol was reviewed and approved by the Animal Use Committee at Hiroshima University.

Monoenergetic neutron irradiation

Various energy neutrons were produced in the Hiroshima University Radiobiological Research Accelerator (HIRRAC) with the ^{7}Li(p,n)^{7}Be reaction. Doses of neutrons and gamma rays were measured at room temperature using paired ionization chambers, IC-17 ATW (FWT Inc. Goleta, CA, USA) or IC-17G (model GM539, FWT Inc. Goleta, CA, USA). The incident neutron energy was calculated by incident proton energy with quantum theory. The incident proton energies were 2.05, 2.2, 2.5 and 2.9 MeV, respectively, then primary energy of produced neutron toward to 30 degrees were 0.254, 0.418, 727 and 1.127 MeV, respectively. According to Lee's theory,[14] the produced neutron energy distribution with thick lithium target can be calculated. Fig. 1 shows the theoretical neutron energy distributions used in following experiments.

Contamination with gamma-rays was less than 3% in the neutron spectrum when using 10 μm-thick ^{7}Li targets. Indi-

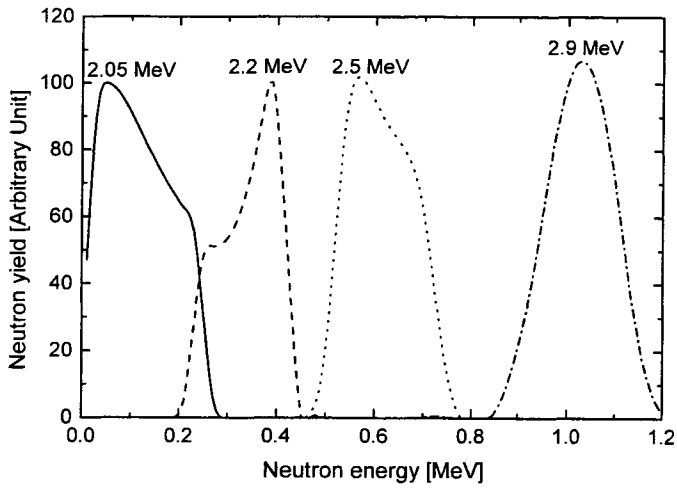

Fig. 1. The neutron energy distribution toward to 30 degrees respect to incident proton beam direction. The distributions are normalized at maximum yield. The energy levels shown on the top of each curve indicate incidence photon energies.

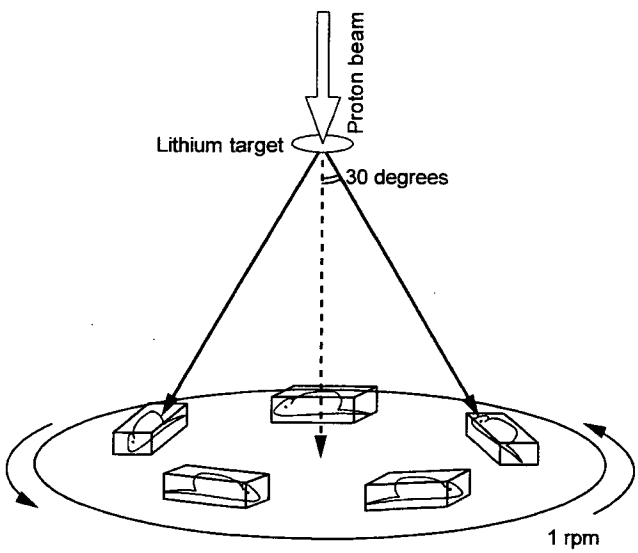

Fig. 2. Experimental setup for neutron irradiation. Five mice were located 20 cm from the neutron producing source at an angle of 30 degrees. In order to provide uniform individual neutron doses, the mice were rotated at a speed of 1 rpm.

vidual mice were placed in individual boxes (3cm × 3cm × 5cm) and groups of 5 mice were located 20 cm from the neutron source at an angle of 30 degrees (Fig. 2) and exposed to monoernergetic neutrons at energy levels of 0.18, 0.32, 0.6 or 1.0 MeV (dose 50cGy, dose rate 0.5cGy/min) without anesthesia. In order to provide uniform individual neutron doses, mice were rotated at a speed of 1 rpm.

Pathology

All animals were regularly observed on a daily basis and weighed once a month. At the time of necropsy, full autopsies were carried out after over ether anesthesia, and body and liver, kidney, adrenal, spleen, testis (male), ovary (female) and uterus (female) weights were determined. The numbers and sizes of liver tumor nodules were also determined and samples of liver and other organs with neoplastic changes were taken and routinely processed for histological examination.

Statistical analysis

The significance of differences in numerical data was determined using 2 × 7 contingency table analysis and the Dunnett's method for multiple comparisons using logarithmic transformation.

RESULTS

Males

Three animals (293, 367 and 362 days after irradiation) died before scheduled autopsy in the 0.18 MeV group, one (365 days) in the 0.32 MeV group, one (319 days) in the 0.6 MeV group and one (403 days) in the 1.0 MeV group. Mean survival period did not significantly differ among the groups. Body weights in the 0.32 MeV group were significantly decreased as compared to control and 1.0 MeV groups. Liver weights with 0.18 MeV were significantly increased as compared with those in control and 0.6 MeV group values, and relative liver weights in the 0.18 MeV group and kidney weights in 0.32 MeV group were elevated (data not shown). There were no other differences in kidney, testis, adrenal and spleen weights among the groups.

Tumor bearing animals accounted for 43% to 60% of the total animals, and the numbers of tumors per animal varied from 0.43 to 0.70. Liver tumors predominated at incidences of 17 to 33%. The number and sizes of liver tumors in the 0.60 MeV group were significantly increased as compared with those in non-irradiated controls but a tendency for decrease was noted with the 1.0 MeV group (see Table 1). There were no significant differences among the irradiated groups. Tumors in sites other than the liver were significantly more frequent in the 0.60 MeV and 1.0 MeV groups than in the controls. Histological findings are summarized in Table 2. Most tumors were rather low in malignancy. However, one osteosarcoma each appeared in the 0.18 MeV and 0.32 MeV groups, one hepatocarcinoma at 0.18 MeV, and 1, 2, and 2 lung adenocarcinomas at 0.18 MeV, 0.32 MeV and 0.6 MeV, respectively. Numbers of hepatomas did not significantly differ among the irradiated groups (Table 2).

Females

Four animals (289, 342, 366 and 388 days after irradiation) died before scheduled autopsy in the 0.18 MeV group, four (219, 276, 366 and 388 days) in the group 0.32 MeV group, three (337, 391 and 419 days) in the 0.6 MeV group, and five (165, 341, 380, 384 and 402 days) in the 1.0 MeV group. There were no differences in the mean survival and